

# TEMPERATURE DEPENDENCE OF THE AGOR MAGNETIC FIELD

L. P. ROOBOL, S. BRANDENBURG, AND H. W. SCHREUDER

*Kernfysisch Versneller Instituut, Zernikelaan 25, NL-9747 AA Groningen, the Netherlands*

It has been found necessary to change the magnet currents gradually during long term operation of the AGOR cyclotron due to temperature changes in the iron, which are caused by the correction coils. These changes influence the magnetization in various ways: through a change in susceptibility, saturation magnetization, and through a change in metal density. Based on long term measurements of the magnetic field as function of temperature, a thermal model has been made, which is compared with theoretical estimates.

## 1 The AGOR magnet

The magnetic field of the AGOR cyclotron is generated mainly by two large superconducting NbTi solenoid pairs. The coils are surrounded by an iron yoke, while the top and bottom of the solenoids are capped with pole pieces reaching almost to the centre of the cyclotron.

The central magnetic field ranges from 1.7 to 4.1 tesla, including a contribution of around 1.5 tesla from the magnetized iron. Small localized corrections to the main field can be made using the fifteen trim coils, which are normal conducting and water cooled.

## 2 Magnetic Drift

In the course of a normal week of operation, AGOR is started up on Monday morning, and turned off on Saturday afternoon. During this time, it was found necessary to gradually change the magnetic field settings of the cyclotron to a higher field value. This effect was linked to temperature changes of the iron of the magnet yoke, shown in Figure 1.

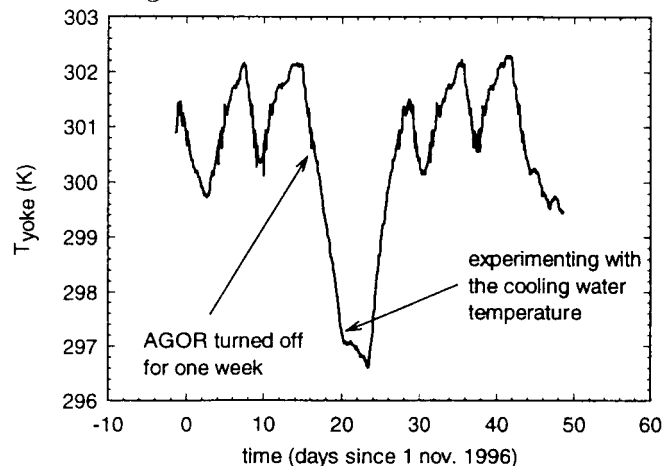


Figure 1: The yoke temperature followed for two months.

Because of an excessive dependence of the temperature of the cooling system on the heat load, the yoke was heated by the cooling water of the (normal conducting)

correction coils. This fact is demonstrated in Figure 2, where we show the behaviour of the field in the centre of the cyclotron, measured with an NMR probe, and the yoke temperature.

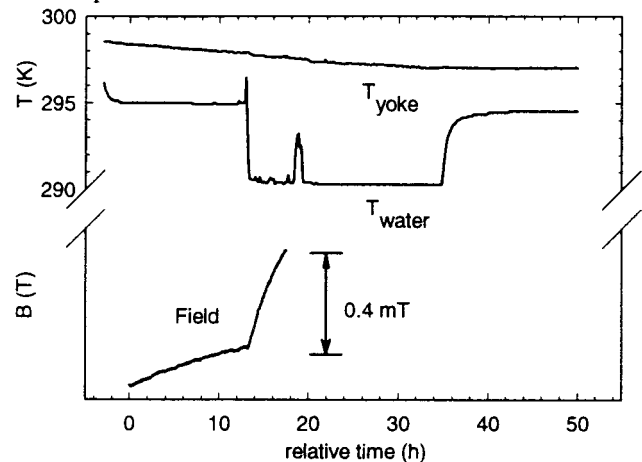


Figure 2: Response of the central field to a step in temperature.

## 3 Temperature and Magnetism

In the following, we consider three temperature dependent effects:

- Finite temperature effects. Because the magnetic phase transition is of second order, the magnetization rises continuously from 0 at  $T_c$  to its saturation value  $M_0$  at absolute zero temperature.
- Volume effects. The specific volume of metals changes with temperature, as does the magnetization density.
- Magnetizing factor effects. When changing volume, the median plane space might change shape, which will affect the magnetic field inside.

### 3.1 Finite temperature

Below a certain critical temperature  $T_c$  (1043 K for iron), the spins in the solid start to align, and magnetization

appears. For a ferromagnetic substance, at absolute zero all the spins are aligned, and maximum magnetization is reached. For temperatures well below  $T_c$ , the temperature dependence of this process was found by Bloch:

$$M(T) = M_0 \left[ 1 - c \frac{1}{nS} (k_B T)^{3/2} \right]$$

Here  $M_0$  is the magnetization at zero temperature,  $n$  is the (number) density of the spins,  $S$  the value of the spin,  $T$  the temperature, and  $c$  a material constant, depending on the (lattice) structure of the material and the coupling between the spins.

For iron, we have

$$\frac{c}{nS} k_B^{3/2} = 3.4 \cdot 10^{-6} \text{ K}^{-3/2}$$

so that the room temperature coefficient of  $M_0$  is  $9 \cdot 10^{-5}$ . We have done measurements at our 190 MeV proton field, where the iron contributes 1.27 T, so that we expect a temperature dependence of  $-0.11 \text{ mT/K}$

Bloch's equation shows that the magnetization is directly influenced by the temperature. There exists an indirect channel as well (through the temperature dependent density), but since this is a second order effect it will be neglected in the following.

### 3.2 Saturation magnetization

At (absolute) zero temperature, the magnetization is just  $M_0 = g\mu_B \frac{N}{V} S$ , with  $g$  the Landé factor (2.219 for iron),  $\mu_B$  the Bohr magneton,  $n = \frac{N}{V}$  the spin (number) density and  $S$  the value of the spin. This expression is not totally temperature independent, because it assumes a constant spin density. To compensate for this effect, one has to introduce a temperature dependent specific volume

$$v(T) = v(T_0) (1 + \gamma(T - T_0))$$

with  $\gamma$  again a material constant, leading to

$$M_0(T) \approx M_0(T_0) (1 - \gamma(T - T_0))$$

The volume expansion coefficient  $\gamma = 3.6 \cdot 10^{-5}$  for iron, which gives us a temperature coefficient of  $-0.05 \text{ mT/K}$  for a 190 MeV proton field.

### 3.3 Magnetizing factor

The magnetic field in the median plane of the magnet is a combination of the field produced by the magnetized iron and the field produced by the coils. The iron contribution ranges from 1.17 out of 1.75 T for the 130 MeV proton beam up to 1.63 out of 4.05 T for a 6 MeV heavy-ion beam with  $Q/A = 0.1$ .

The iron field scales of course with the magnetization, but also the shape of the gap between the poles comes

into play. For a cyclotron gap geometry where most of the surface of the gap is perpendicular to the magnetic field, the field inside the hole is equal to the field in the material.

In the approximation that the whole of the magnet expands and contracts isotropically with a change in temperature, the shape of the gap does not change, only its size, which means that the magnetic field will not change due to this effect.

### 3.4 Theoretical conclusion

Adding the two effects of significance, we expect a thermal coefficient of the magnetic field of about  $-0.16 \text{ mT/K}$ .

## 4 Measurements of drift

We have also tried to quantify the temperature drift of the magnetic field. In one case the temperature of the iron was changed while measuring the central field with a NMR probe. In another case we tried to measure the change indirectly, by plotting the change in beam phase induced by different magnet settings against the temperature of the yoke.

### 4.1 Central field: NMR

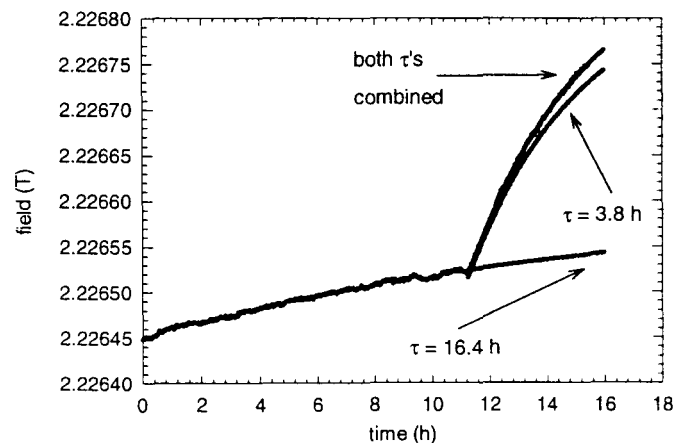


Figure 3: Temperature drift in more detail.

Figure 3 shows the rise in field of figure 2 in more detail. It is clear that we see a sum of at least two exponential relaxations, a fast one with a time constant of approximately 4 hours, associated with the change in cooling water temperature, and a slower one, of about 16 hours.

From the exponential function with the 4 hour time constant, we fitted the field step which was the effect of a rise in temperature of 4.5 K. The field rise due to the temperature step was  $0.32 \text{ mT}$ , which gives us a linear temperature dependence of  $-0.07 \text{ mT/K}$ .

## 4.2 Beam phase at extraction

Another type of measurement is to correlate the magnet settings needed to produce a certain beam with the temperature of the magnet yoke. One assumes that the beam phase at extraction radius is adjusted to be constant, and calculates the effect on  $\sin\varphi$  of the deviation in the magnet settings. The result of such a calculation for our 189 MeV proton beam is shown in figure 4. The line is a least squares fit with slope  $0.24\text{ K}^{-1}$ .

According to Gordon, this beam phase (at extraction radius  $R$ ) is given by

$$\Delta \sin \varphi = K \int_0^R \gamma^2(r) \frac{\Delta B}{B_0} dr^2$$

The constant  $K$  contains information on RF frequency and the acceleration voltage,  $B_0$  is the central magnetic field,  $\Delta B$  is the deviation from the isochronous field, and  $\gamma$  is the relativistic mass enhancement factor.

For a uniform  $\Delta B$ , this integral can be solved and gives  $\Delta \sin \varphi = 2.5 \cdot 10^3 \Delta B$  for our 189 MeV proton beam. Accepting the fitted value of  $0.24\text{ K}^{-1}$  we derive a temperature coefficient of  $\Delta B / \Delta T = -0.10\text{ mT/K}$ .

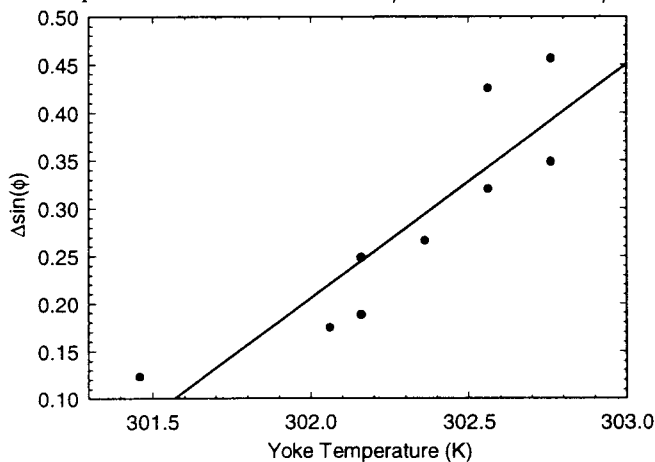


Figure 4: Beam phase at extraction as function of temperature.

## 4.3 Experimental conclusions

The temperature coefficient of the central field as measured by NMR is  $-0.07\text{ mT/K}$ . Using the indirect method of comparing magnet settings, we find good correlation of the beam phase at extraction with the yoke temperature, and an associated temperature coefficient of  $-0.10\text{ mT/K}$ . These values are in reasonable agreement with each other.

## 5 Thermal model

Figure 5 shows a model of the thermal connections between the various parts of the magnet. The trim coils are

wound round banana shaped iron pieces, which are connected through some metal blocks to the magnet yoke. The water cooling the trim coils is led through copper pipes of rectangular cross section, clamped in between the 'bananas' and the 'blocks', with about equal surface area to either side.

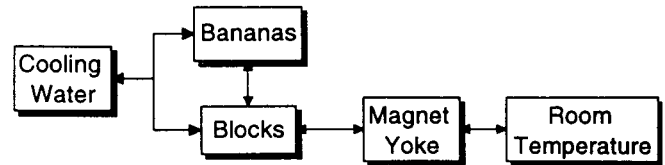


Figure 5: Thermal diagramme of the magnet.

The iron closest to the beam are the bananas, which have a total mass of 1.44 tonnes and with them we associate the thermal time constant of 3.8 hours found in the NMR measurements. The blocks on which they are resting have a mass of 6.5 tonnes and an associated time constant of 16 hours.

The fact that the ratio of the time constants equals the ratio of the masses indicates that the thermal resistance of these components to the cooling water is equal. During two weeks in 1996, the cyclotron was turned off, and the yoke temperature started to relax to its equilibrium value. From this cool down period, we estimate the thermal relaxation time constant of the magnet yoke to be about 70 hours. This is 4.4 times longer than the time constant of the blocks, while the mass of the yoke is 28 times larger. This means the thermal conductivity between the blocks and the yoke should be about 6 times better than the conductivity between the blocks and the cooling water.

## 6 Conclusions

The sum of the contributions to the temperature coefficient of the field is

$$\frac{\partial B}{\partial T} = -0.16\text{ mT/K}$$

while the experimental values were  $-0.07$  and  $-0.10\text{ mT/K}$ .

The discrepancy can be due to the fact that there are large error bars on the amplitude of the field excursion in figure 3, because we did not have enough data to fit the whole exponential decay.

The beam phase plot did give a similarly low value for the temperature coefficient, but this could be due to the fact that the yoke temperature is connected to the temperature of the "bananas" through a very long time constant, which can skew measurements.

Concludingly, we remark that temperature stabilization of the magnet would remove one of the last remaining sources of non-reproducibility in modern cyclotrons.

Great care should be taken while measuring field maps, since differences in temperature could easily cause errors up to  $0.5 \text{ mT}$ .

Also, the iron temperature should be taken into account when calculating magnet settings to produce a certain beam.

## References

- [1] Neil W. Ashcroft and N. David Mermin, *Solid State Physics*, (Holt Saunders International Editions, Philadelphia, U.S.A., 1981).
- [2] R. P. Feynman, R. B. Leighton, and M. Sands, *the Feynman lectures on physics*, (Addison-Wesley publishing company, Reading, U.S.A., 1963).
- [3] M. N. Wilson, *Superconducting Magnets*, (Oxford university press, Oxford, U.K., 1983).